05

Controlled modes of spin-wave signal propagation in lateral YIG microwaveguides with an orthogonal element

© R.V. Masliy, A.B. Khutieva, A.V. Sadovnikov

Saratov National Research State University,
Saratov, Russia

E-mail: romamaslij5@gmail.com

Received April 18, 2024
Revised April 18, 2024
Accepted May 8, 2024

The propagation of spin waves (SWs) in a structure consisting of two waveguides arranged in the horizontal plane with a gap between them and one waveguide positioned above and perpendicular to them is analyzed. The method of micromagnetic modeling is used to identify the mechanism for controlling the spatial structure of a spin-wave beam and its splitting between channels of an array of microwaveguides based on yttrium iron garnet (YIG). Specifically, it is demonstrated that the direction of propagation of SWs in the array may be altered by adjusting the frequency fed to the central channels of one of the layers. The power concentration modes for a signal encoded as the amplitude and phase of SWs at the ends of the central channels with the possibility of their separate activation and control over the signal at the ends of microwaveguides of the upper array layer are examined in detail. A microwaveguide array of this kind may thus be regarded as a controlled logic device or a multichannel power divider.

Keywords: spin wave, micromagnetic modeling, nonreciprocity, spin-wave beam.

DOI: 10.61011/PSS.2024.08.59040.54HH

1. Introduction

When used instead of charge transfer, the transfer of magnetic moment or spin of an electron opens up new opportunities for application of quantum spin-wave excitations (e.g., magnons) in the development of methods and approaches for processing, transmission, and storage of signals encoded as the amplitude and phase of spin waves (SWs) in the microwave and terahertz ranges [1–9]. The lengths of excited SWs range from hundreds of micrometers to tens of nanometers and may vary under the influence of various factors, such as the magnitude and direction of the magnetization field, the type and magnitude of anisotropy of the magnetic material, and irradiation of the surface of magnetic films with focused laser radiation.

The record-low attenuation of SWs in films made of ferromagnets based on yttrium iron garnet (YIG) is the basis for study of spin transfer processes in structured films. The branch of physics of magnetic phenomena and condensed matter physics concerned with these processes is known as dielectric magnonics [9]. YIG is used as a material and medium for studying processes that affect the characteristics of SWs (magnitude and direction of the group velocity of SWs, spatial distribution of their amplitude and phase, and frequency ranges of excitation and propagation of SWs) and various methods for control over SW coupling in multilayer structures and other systems. The feasibility of application of YIG-based structures as elements of logic devices operating in the microwave range was demonstrated in certain studies [10–13]. Planar ferrite waveguide microstructures based on YIG may be used as basic elements of „magnonic networks“ for various signal processing devices (delay lines, filters, interferometers, switches, multiplexers, etc. [13–16]). Data is transmitted in these devices via spin waves, and logical operations are implemented based on spin-wave interference. The use of lateral magnetic microstructures is important for the development of connection elements in planar topologies of magnonic networks [10]. Frequency tuning and output signal parameters in such microstructures are controlled by adjusting the effective dielectric and magnetic permeability of a layered structure under the influence of external electric and magnetic fields, respectively. However, the fabrication of such structures requires precise alignment of piezoelectric layers on the surface of waveguides or matching in the process of ion-beam deposition onto the surface of piezoelectric or semiconductor substrates. The study of multilayer structures containing a microwaveguide system allows one to examine the ways to control the spectra of spin waves and signal propagation modes by adjusting the distance between individual waveguides and between the system layers. This method of controlling the signal splitting between channels extends the functionality of magnonic structures used in parallel processing of data signals [17–21].

Thus, the present study is focused on finding the methods for control over the amplitude and phase of SWs in multilayer structures with each of their layers formed by magnonic microwaveguides. The base case with one layer containing magnonic microwaveguides positioned on the same substrate and spaced by a distance comparable to the thickness of the magnetic material was considered.

This helped establish the mode of dipole coupling of spin waves in planar laterally oriented structures. A magnonic microwaveguide of the same width oriented orthogonally to the system of lateral microwaveguides was located in the second layer. This allowed us to implement spin-wave transport controlled by the magnetic field orientation. A detailed analysis of SW propagation modes in the composite structure was carried out to reveal the specifics of SW propagation. The effect of dipole coupling of SWs propagating in parallel ferrite strips and coupling with the orthogonal microwaveguide positioned above them was investigated via micromagnetic modeling. Anisotropic signal propagation, dipole-dipole coupling, and the nonlinear frequency dependence of parameters of the medium in a system of coupled microwaveguides shaping the SW propagation modes were taken into account. Methods for controlling the spatial structure of a spin-wave beam and its splitting between channels of a microwaveguide array were proposed and studied. It was found that the direction of propagation of spin waves in the array may be altered by adjusting the frequency fed to the central channels of one of the layers. The power concentration modes for a signal encoded as the amplitude and phase of spin waves at the ends of the central channels with the possibility of their separate activation and control over the signal at the ends of microwaveguides of the upper array layer were also examined in detail. The availability of a large number of ports and two layers for processing the received data opens up opportunities for application of this microwaveguide array as a controlled logic device or a multichannel power divider.

2. Structure under study and numerical model

Micromagnetic modeling of a system consisting of laterally ($A_{1,2}$) and vertically (A_3) coupled ferrite microwaveguides made of an yttrium iron garnet film and positioned on a gadolinium gallium garnet (GGG) substrate was carried out. The microwaveguides had the form of elongated strips with the following dimensions: length $L = 6$ mm, width $c = 300\,\mu$m, and thickness $b = 10\,\mu$m. The structure consisted of two waveguides arranged horizontally with a small gap between them [22] and one waveguide positioned above and perpendicular to them [3] (see Figure 1).

YIG was in a single-domain state. The saturation magnetization of YIG was $M = 139$ G, and external magnetic field $H = 1200$ Oe was directed along the y axis. The numerical study was carried out within the 5.15–5.35 GHz frequency range. Efficient excitation of surface spin waves was established in this configuration and at these frequencies, providing for an expansion of functional capabilities of microwave devices. The specific feature of coupled ferrite structures is the capacity for control over coupling between the width modes of spin waves [22–25] propagating in individual ferromagnetic microwaveguides, which adds an additional control parameter. The mumax^3 [26] simulation program was used for numerical modeling. It allows one to solve numerically the Landau–Lifshitz equation with attenuation in the form of a Hilbert phenomenological term. This approach is commonly applied to problems of excitation and propagation of SWs in magnonic structures [3–9].

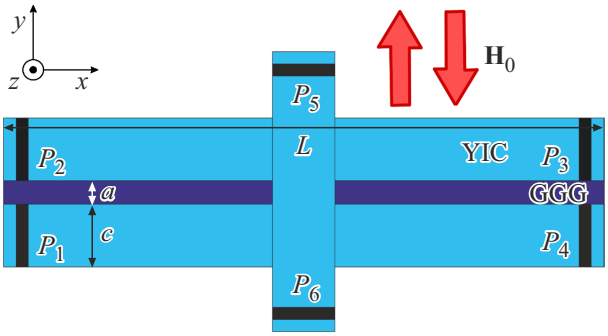

Figure 1. Schematic diagram of the microwaveguide array. The following notation is introduced here: a — horizontal gap; c — width; L — length of microwaveguides; $P_{1,2}$ and P_{3-6} — microstrip antennas for excitation and reception of SWs, respectively.

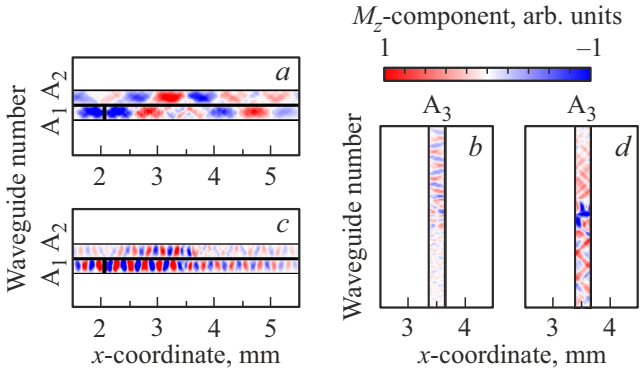

Figure 2. Spatial distribution maps of the M_z component of dynamic magnetization for SWs propagating in the microwaveguide array. (a, b) — Excitation of a wave at a frequency of 5.15 GHz; (c, d) — excitation of a wave at a frequency of 5.35 GHz.

3. Results of micromagnetic modeling of propagation modes of spin waves in an array of YIG strips

The SW source is shown in Figure 2 in the form of a black rectangle positioned on microwaveguide A_1. The propagation of an SW excited at a frequency of 5.15 and 5.35 GHz in waveguides A_1–A_2 of the lower layer is shown in Figures 2, a and c, and its propagation in waveguide A_3 of the upper layer is illustrated in Figures 2, b and d, respectively. The dynamics of SW propagation in laterally and vertically coupled waveguides was investigated by plotting maps of the spatial distribution of dynamic magnetization.

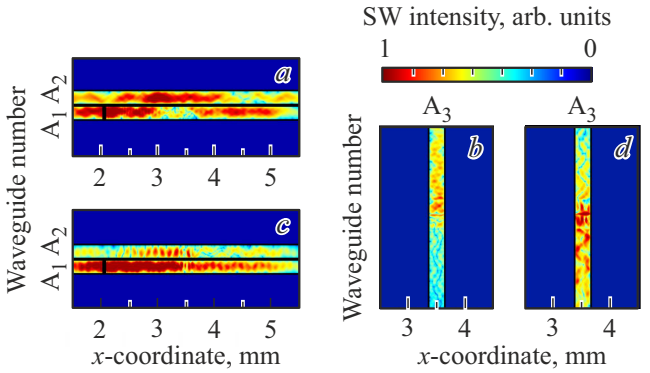

Figure 3. Spatial distribution of SW intensity $I(x, y)$ represented by color gradient. (a, b) — Excitation of a wave at a frequency of 5.15 GHz; (c, d) — excitation of a wave at a frequency of 5.35 GHz.

Figure 2 presents a stationary settling pattern of the wave process with propagation observed both into the adjacent microwaveguide from the same layer and in the vertical direction. In the first case (Figure 2, *a*), the wavelength is 500 μm; with the same design and a frequency of 5.35 GHz (Figure 2, *c*), the wavelength is 250 μm. It should be noted that the upper waveguide exerts virtually no influence on the wavelength and its propagation. Having examined the wave evolution in waveguide A_3, one may identify the propagation mode of a backward volume SW [3]. Its wavelength in the case of propagation in the positive direction of axis y exceeds the wavelength of an SW propagating in the negative direction of axis y. The multimode nature of an SW in section A_3, which is manifested in simultaneous propagation of the first and second width modes of a backward volume magnetostatic wave [23–25], should be noted. At different frequencies (in the present case, 5.15 and 5.35 GHz), the spatial SW amplitude profiles are specified by different contributions of the first or second width modes. In Figures 2, *a* and *c*, the wave propagates along the external field **H** vector, but propagation in Figures 2, *b* and *d* is directed opposite to the direction of the external field.

Let us examine the processes of formation of spin-wave signal beams by plotting the spatial distribution of SW intensity. Figures 3, *a* and *c* present the propagation of waves in waveguides A_1-A_2 of the lower layer, while Figures 3, *b* and *d* illustrate the wave propagation in

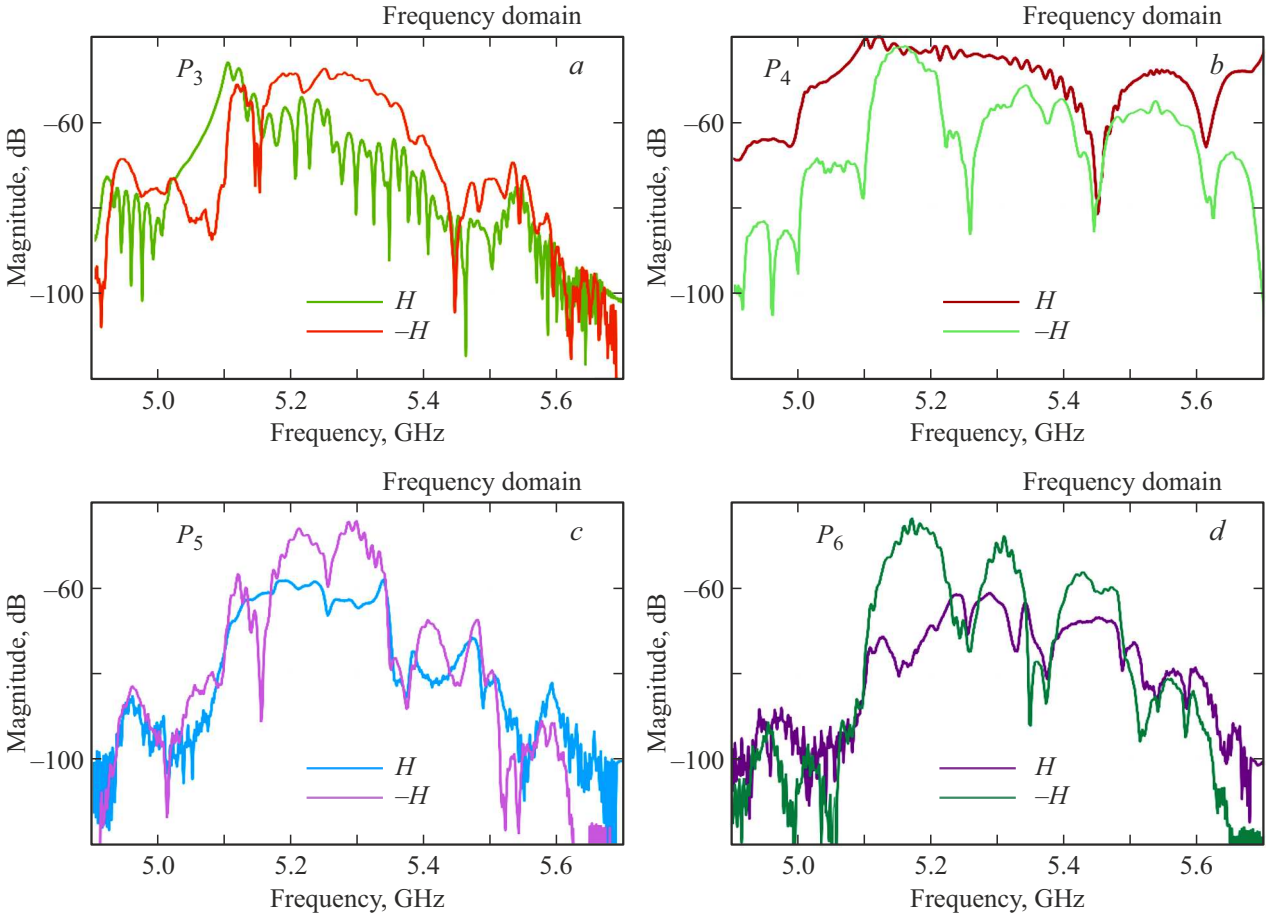

Figure 4. Amplitude-frequency response at the output ports of the structure plotted via micromagnetic modeling with reversal of the magnetic field orientation. The designations of the output ports are indicated in each panel. The magnitude of the external magnetic field was 120 Oe in all cases.

waveguide A_3 of the upper layer at time point $t = 200$ ns after the establishment of a stationary SW propagation mode. The length of power transfer due to the SW coupling is 1 mm for Figure 3, *a*, while no pronounced power transfer is seen in Figure 3, *c*.

Frequency dependences of the spectral power density under varying orientation of the magnetization field were plotted in order to identify the modes of nonreciprocal propagation of SWs in the studied structure. Specifically, a pulse signal was set at the input antenna, and the Fourier transform was performed to construct spectra at the output antennas corresponding to each of the output ports P_{3-6} of the structure. The obtained spectra (Figure 4) demonstrate that the magnetization field reversal has a pronounced influence on the level of transmission of the spin-wave signal to the output ports of the structure. For example, examining the signal from the P_4 port, one may note a change in the number and depth of dips caused by the transfer of spin-wave power between microwaveguides A_1 and A_2. This is attributable to the nonreciprocal nature of the surface magnetostatic wave, which is induced by a change in the SW amplitude profile in the direction orthogonal to the film surface (axis z in Figure 1). At the same time, a profound change in the output signal spectrum is observed for orthogonally positioned microwaveguide A_3, although the nonreciprocity properties are, as is commonly known, not manifested for a backward volume wave that propagates in A_3. Thus, the proposed structure in combination with the method of control by reversing the magnetization field orientation may be used as a microwave signal filter, a controlled demultiplexer, or a magnonic element for logic devices.

4. Conclusion

The dual control of SW characteristics in an array of YIG microwaveguides with simultaneous lateral and vertical coupling was investigated. The features of formation of SW beams in coupled magnetic waveguides were examined. The propagation specifics and mechanisms of variation of the spatial distribution of the spin-wave beam profile were identified. A change in the nature of SW power localization in the linear mode in the output sections of microwaveguides was revealed by examining the obtained spatial distributions of the dynamic SW magnetization components. The proposed method for controlling the SW properties may be used in multilayer topologies of magnonic networks and magnonic logic devices based on them.

Funding

This study was supported financially by the Russian Science Foundation, project No. 20-79-10191.

Conflict of interest

The authors declare that they have no conflict of interest.

References

[1] S.A. Nikitov, D.V. Kalyabin, I.V. Lisenkov, A.N. Slavin, Y.N. Barabanenkov, S.A. Osokin, A.V. Sadovnikov, E.N. Beginin, M.A. Morozova, Y.P. Sharaevsky, Y.A. Filimonov, Y.V. Khivintsev, S.L. Vysotsky, V.K. Sakharov, E.S. Pavlov. Phys. — Usp. **58**, *10*, 1002 (2015).
[2] V.E. Demidov, S. Urazhdin, A. Zholud, A.V. Sadovnikov, A.N. Slavin, S.O. Demokritov. Sci. Rep. **5**, *1*, 8578 (2015).
[3] C.S. Davies, A. Francis, A.V. Sadovnikov, S.V. Chertopalov, M.T. Bryan, S.V. Grishin, D.A. Allwood, Y.P. Sharaevskii, S.A. Nikitov, V.V. Kruglyak. Phys. Rev. B **92**, *2*, 020408(R) (2015).
[4] A.V. Sadovnikov, E.N. Beginin, S.E. Sheshukova, Yu.P. Sharaevskii, A.I. Stognij, N.N. Novitski, V.K. Sakharov, Yu.V. Khivintsev, S.A. Nikitov. Phys. Rev. B **99**, *5*, 054424 (2019).
[5] A.V. Sadovnikov, A.A. Zyablovsky, A.V. Dorofeenko, S.A. Nikitov. Phys. Rev. Appl. **18**, *2*, 024073 (2022).
[6] M. Balynsky, D. Gutierrez, H. Chiang, A. Kozhevnikov, G. Dudko, Y. Filimonov, A.A. Balandin, A. Khitun. Sci. Rep. **7**, *1*, 11539 (2017).
[7] A.B. Ustinov, A.V. Drozdovskii, B.A. Kalinikos. Appl. Phys. Lett. **96**, *14*, 142513 (2010).
[8] L.A. Shelukhin, V.V. Pavlov, P.A. Usachev, P.Yu. Shamray, R.V. Pisarev, A.M. Kalashnikova. Phys. Rev. B **97**, *1*, 014422 (2018).
[9] S.A. Nikitov, A.R. Safin, D.V. Kalyabin, A.V. Sadovnikov, E.N. Beginin, M.V. Logunov, M.A. Morozova, S.A. Odintsov, S.A. Osokin, A.Yu. Sharaevskaya, Yu.P. Sharaevsky, A.I. Kirilyuk. Phys. — Usp. **63**, *10*, 945 (2020).
[10] A.Yu. Annenkov, S.V. Gerus, S.I. Kovalev. Tech. Phys. **43**, *2*, 216 (1998).
[11] Y.K. Fetisov, G. Srinivasan. Appl. Phys. Lett. **88**, *14*, 143503 (2006).
[12] S.L. Vysotskiy, Yu.V. Khivintsev, V. Sakharov, Yu. Filimonov. Tech. Phys. **64**, *7*, 984 (2019).
[13] A.A. Grachev, A.V. Sadovnikov, S.A. Nikitov. Nanomater. **12**, *9*, 1520 (2022).
[14] A. Stognij, L. Lutsev, N. Novitskii, A. Bespalov, O. Golikova, V. Ketsko, R. Gieniusz, A. Maziewski. J. Phys. D **48**, 485002 (2015).
[15] A.I. Stognij, L.V. Lutsev, V.E. Bursian, N.N. Novitskii. J. Appl. Phys. **118**, *2*, 023905 (2015).
[16] G. Gubbiotti, A. Sadovnikov, E. Beginin, S. Nikitov, D. Wan, A. Gupta, S. Kundu, G. Talmelli, R. Carpenter, I. Asselberghs, I.P. Radu, C. Adelmann, F. Ciubotaru. Phys. Rev. Appl. **15**, *1*, 014061 (2021).
[17] A.K. Ganguly, C. Vittoria. J. Appl. Phys. **45**, *10*, 4665 (1974).
[18] H. Puszkarski. Surf. Sci. Rep. **20**, *2*, 45 (1994).
[19] M.R. Daniel, P.R. Emtage. J. Appl. Phys. **53**, *5*, 3723 (1982).
[20] A.V. Sadovnikov, E.N. Beginin, S.E. Sheshukova, D.V. Romanenko, Yu.P. Sharaevskii, S.A. Nikitov. Appl. Phys. Lett. **107**, *20*, 202405 (2015).
[21] A.Y. Annenkov, S.V. Gerus, E.H. Lock. Europhys. Lett. **123**, *4*, 44003 (2018).
[22] A.B. Khutieva, A.V. Sadovnikov, A.Yu. Annenkov, S.V. Gerus, E.H. Lock. Bull. Russ. Acadmy. Sci.: Phys. **85**, *11*, 1205 (2021).

[23] S.N. Bajpai. J. Appl. Phys. **58**, *2*, 910 (1985).
[24] T.W. O'Keeffe, R.W. Patterson. J. Appl. Phys. **49**, *9*, 4886 (1978).
[25] O. Buttner, M. Bauer, C. Mathieu, S.O. Demokritov, B. Hillebrands, P.A. Kolodin, M.P. Kostylev, S. Sure, H. Dotsch, V. Grimalsky, Y. Rapoport, A.N. Slavin. IEEE Trans. Magn. **34**, *4*, 1381 (1998).
[26] A. Vansteenkiste, J. Leliaert, M. Dvornik, M. Helsen, F. Garcia-Sanchez, B. Van Waeyenberge. AIP Adv. **4**, *10*, 107133 (2014).

Translated by D.Safin